Bound states of the barium atom by the hyperspherical approach

M. A. Cebim and J. J. De Groote

Citation: The Journal of Chemical Physics **121**, 11129 (2004); doi: 10.1063/1.1817911
View online: http://dx.doi.org/10.1063/1.1817911
View Table of Contents: http://scitation.aip.org/content/aip/journal/jcp/121/22?ver=pdfcov
Published by the AIP Publishing

Bound states of the barium atom by the hyperspherical approach

M. A. Cebim[a)]
Instituto de Química de Araraquara, Universidade Estadual Paulista—UNESP, Caixa Postal 355, 14801-970 Araraquara, São Paulo, Brazil

J. J. De Groote
Laboratório de Inteligência Artificial e Aplicações, Faculdades COC, Rua Abraão Issa Halack 980, 14096-175 Ribeirão Preto, São Paulo, Brazil

(Received 25 May 2004; accepted 24 September 2004)

We present a nonadiabatic hyperspherical calculation of the highly excited and low lying doubly excited states of the barium atom using effective potentials for the two optically active electrons' interactions. Within the hyperspherical adiabatic approach the investigation of the spectra is performed with potential curves and nonadiabatic couplings of a unique radial variable, which allows clear identification of the states. The convergence of energy is obtained within well established bound limits, and the precision is comparable to accurate configuration interaction calculations. A very good agreement with experimental results is obtained with only few nonadiabatic couplings. © *2004 American Institute of Physics.* [DOI: 10.1063/1.1817911]

I. INTRODUCTION

Alkali and alkaline-earth atoms have been studied in the last years following the developments on the laser spectroscopy.[1,2] A detailed analysis of the spectra by theoretical methods becomes important, and different approaches have been applied. As an alternative to the many-electron treatment of the alkali atoms, the effective potentials for the valence electrons have been considered with good results. Not only precise bound state energies[3] have been calculated but also the excited and resonant ones.[4] These results, usually obtained using the configuration interaction (CI) framework, show an important dependence on the electronic correlation. To deal with this aspect we present a hyperspherical (HS) adiabatic approach (HAA) calculation, based on the efficiency obtained for strong correlated two-electron systems.[5–28]

The HS method was introduced for the atomic physics in the 1960s,[5] bringing a new perspective for the helium atom doubly excited states analysis. Since the first qualitative results, fast convergent approaches have been developed with precise results for two- and three-electron systems, with results ranging from autoionizing states to precise highly excited states.[22,26,27]

In this work, the Schrödinger equation of the barium atom using a model potential is solved by means of a nonadiabatic hyperspherical approach. This method has also been chosen in order to proportionate an alternative insight to the variational or the multiconfiguration Hartree–Fock approach followed by the CI procedure. With Born–Oppenheimer-like, one radial variable potential curves, the HAA is an important tool to identify both bound and resonant states. The adiabatic procedure also allows lower and upper bounds for the exact Schrödinger equation ground state energy using only uncoupled HS radial equations. Even within this simple approximation, for most of the two-electron systems studied with this approach, the ground state have good precision, with errors usually inferior to 3%.[16] Through the nonadiabatic procedure the error decreases as more radial channels are coupled in the HS radial equation. For the sodium atom, three coupled channels are enough for electron affinity calculation error below 0.1%.[28]

The HAA is an *ab initio* procedure with approximations due to the truncation on the number of coupled second order ordinary differential equations and the usual numerical floating point error propagation. It is based on the hyperspherical coordinates R and α, which correlates the electronic radial variables r_1 and r_2 in a transformation similar to the bidimensional Cartesian to the polar one, $R\sin\alpha=r_1$, $R\cos\alpha=r_2$. The resulting new set of coordinates is formed by five compact ones, the four original electronic spherical angular and only one radial. The adiabatic procedure separates the Schrödinger partial differential equation into an R dependent HS angular equation, whose eigenvalues form potential curves, and a coupled system of ordinary radial differential equations. All terms from the particles interaction potentials are contained within the HS angular equation, which means that good quality solutions are required to correctly account for their contribution. In this work we solve the coupled angular equations with a variable step numerical propagation method. The number of coupled terms is chose considering the desired precision, which is straightforward since the convergence is directly related to the number of angular momenta configurations taken into account. With the potential curves determined, the HS angular eigenstates, the so-called channel functions, are used to generate the HS radial nonadiabatic couplings. These couplings reflect the quality of the HS angular solutions since first- and second-order derivatives of the channel functions with respect to R are involved. Otherwise, small fluctuations derived from numerical errors would be amplified, affecting the results.

An important characteristic of the HS angular solutions

a)Electronic mail: maccebim@posgrad.iq.unesp.br

is their independence from the energy. Once the potential curves and nonadiabatic couplings have been calculated, all the properties related to the energy will be relative to the radial equation eigenstates. In this respect it is important to notice the practical aspect that all bound states within a potential curve are obtained from the same equation, without any adjustable parameter and without the need to impose the eigenstates orthogonalization, as required by variational approaches.

In Sec. II we briefly present the hyperspherical adiabatic approach for the barium atom and the model potential (Sec. II A), followed by the hyperspherical angular solutions (Sec. II B). Section III is devoted for results and discussion, and in Sec. IV the conclusions are presented. Atomic units are used throughout the paper.

II. THE HYPERSPHERICAL COORDINATE METHOD

A. Hyperspherical adiabatic approach

The Schrödinger equation of a two-electron system bound to a nucleus at fixed position is given by

$$\left[-\nabla_1^2-\nabla_2^2+\frac{2}{|\vec{r}_1-\vec{r}_2|}+\mathcal{U}(r_1)+\mathcal{U}(r_2)-2E\right]\Psi(\vec{r}_1,\vec{r}_2)=0. \tag{1}$$

The effective potentials $\mathcal{U}$ for the electrons, using the model potential developed by Féret and Pascale[4] for the barium atom are defined as

$$\mathcal{U}(r)=-\frac{Z-N}{r}+V^{\mathrm{LR}}(r)+\sum_{\ell=0}^{\infty}V_\ell^{\mathrm{SR}}\sum_{m=-\ell}^{\ell}|\ell m\rangle\langle\ell m|, \tag{2}$$

which contains a nonlocal long-range contribution $V^{\mathrm{LR}}(r)$,

$$V^{\mathrm{LR}}(r)=-\frac{a}{4r^4}[f(r)]^2, \tag{3}$$

and a semilocal short-range potential,

$$V_\ell^{\mathrm{SR}}(r)=(a_\ell+b_\ell r+c_\ell r^2)\frac{\exp(-\beta_\ell r^p)}{r^q}. \tag{4}$$

These potentials describe core polarization effects, accounting for the loss of core symmetry due to the action of the valence electron field, and also the partial screening of the nucleus.

The cutoff function

$$f(r)=\frac{r^3}{r^3+r_c^3} \tag{5}$$

is set to provide the correct short-range behavior of the nonlocal potential term, with r_c chosen to be approximately the core radius.

The introduction of the hyperspherical coordinates R and α,

$$R^2=r_1^2+r_2^2, \tag{6}$$

$$\tan\alpha=\frac{r_1}{r_2}, \tag{7}$$

correlates the electronic spherical radial variables. The new set of compact coordinates is $\Omega=(\alpha,\theta_1,\theta_2,\phi_1,\phi_2)$, with the four original electronic spherical angular. Only R is radial.

The new Schrödinger equation then reads,

$$\left[\frac{\partial^2}{\partial R^2}+\frac{1}{4R^2}+\frac{1}{R^2}\hat{U}(R,\Omega)+2E\right]\times(R^{5/2}\sin\alpha\cos\alpha)^{-1}\psi(R,\Omega)=0. \tag{8}$$

The hyperspherical angular operator $\hat{U}(R,\Omega)$ is not separable with respect to the hyperradius R, since contains the potential energy terms,

$$\hat{U}(R,\Omega)=\frac{\partial^2}{\partial\alpha^2}-\frac{L_1^2}{\sin^2\alpha}-\frac{L_2^2}{\cos^2\alpha}-2R^2V(R,\Omega), \tag{9}$$

where $\cos\theta_{12}=\hat{r}_1\cdot\hat{r}_2$, and,

$$V(R,\Omega)=\mathcal{U}(R\sin\alpha)+\mathcal{U}(R\cos\alpha)-\frac{2R}{\sqrt{1-\sin 2\alpha\cos\theta_{12}}}. \tag{10}$$

Within the hyperspherical adiabatic approach the equation for $\hat{U}(R,\Omega)$ is solved for fixed values of R,

$$\hat{U}(R,\Omega)\Phi_\mu(R;\Omega)=U_\mu(R)\Phi_\mu(R;\Omega). \tag{11}$$

The eigenvalues $U_\mu(R)$ are potential curves and the eigenfunctions Φ_μ, the so-called channel functions,[18] form a basis set for the total wave function as

$$\psi(R,\Omega)=\sum_\mu F_\mu(R)\Phi_\mu(R;\Omega). \tag{12}$$

The expansion coefficients F_μ and the system energy are determined from the HS radial equation,

$$\left(\frac{\partial^2}{\partial R^2}+2E+\frac{U_\mu(R)+1/4}{R^2}\right)F_\mu(R)+\sum_v\left(2P_{\mu v}(R)\frac{\partial}{\partial R}+Q_{\mu v}(R)\right)F_v(R)=0, \tag{13}$$

obtained substituting the wave function expansion into the HS Schrödinger equation. This is an infinite set of differential equations coupled by the nonadiabatic terms,

$$P_{\mu v}(R)=\langle\Phi_\mu|\frac{\partial}{\partial R}|\Phi_v\rangle, \tag{14}$$

$$Q_{\mu v}(R)=\langle\Phi_\mu|\frac{\partial^2}{\partial R^2}|\Phi_v\rangle, \tag{15}$$

where the brackets represent integration over the angular variables Ω.

For an initial approximation, all the couplings may be disregarded, leading to simple uncoupled second order differential equations. The energies obtained from such equations [extreme uncoupled adiabatic approach (EUAA)] will be lower energy levels if the HS potential wells are deep enough to allow bound states. A sensible improvement to this

simple approximation, the UAA (uncoupled adiabatic approach), which gives upper bounds for the exact system energy, is determined by the introduction of the diagonal couplings. The efficiency of the adiabatic approach is related to the small corrections of the nonadiabatic couplings to the energy levels. As the nondiagonal couplings are gradually introduced within the CAA (coupled adiabatic approach) the binding energies approach the exact solution of the Schrödinger equation as

$$E_{\mathrm{EAA}}<E\leqslant E_{\mathrm{CAA}}<E_{\mathrm{UAA}}. \tag{16}$$

B. The hyperspherical angular solutions

The precise calculation of the angular channel basis is an important requirement for the efficiency of the adiabatic expansion. The HS radial equations for different three-body systems will only differ by the potential curves and couplings, which embodies the system characteristics, since the HS angular operator contains all interaction terms [cf. Eq. (9)].

For heliumlike potential terms, the HS angular equations may be solved analytically[10] by a power series expansion with the variable change $z=\tan(\alpha/2)$. For the model potential used in this work, this approach is no longer possible due to the slow convergence of the exponential and cutoff functions power series expansion. Therefore, we proceed with a numerical approach, the step variable Bulirsch–Stoer method,[29] although other variable step methods may also be applied with good results.

The potential interaction terms in the HS angular equation are cancelled when $R=0$. This means that for small values of R, the kinetic HS angular operator eigenstates, the hyperspherical harmonics,[22]

$$\Phi_{\mu}(R;\Omega)=\sum_{l_1 l_2}(\sin\alpha)^{l_1+1}(\cos\alpha)^{l_2+1}P_{\mu l_1 l_2}(\alpha)\times\mathcal{Y}^{\mathrm{LM}}_{l_1 l_2}(\Omega_1,\Omega_2), \tag{17}$$

predominate, representing the behavior of the two electrons close to the nucleus. For large values of R, one of the electrons is bound close to the nucleus while the other is further away, in the field of a resulting potential of the core screened by the inner electron. In this case the angular channel reflects, in first order, a hydrogenic wave function, while the potential curve value approaches the ionized system Ba^+ energy.

In order to improve the convergence of the HS angular solutions, the wave function is adjusted by the introduction of the small and large R behavior as,

$$\Phi_{\mu}(R;\Omega)=N_{\mu}\sum_{l_1 l_2}G_{\mu l_1 l_2}(R;\alpha)\mathcal{Y}^{\mathrm{LM}}_{l_1 l_2}(\Omega_1,\Omega_2), \tag{18}$$

where N_{μ} is a normalization constant and $\mathcal{Y}^{\mathrm{LM}}_{l_1 l_2}(\Omega_1,\Omega_2)$ are the coupled spherical harmonics, with $|l_1-l_2|\leqslant L\leqslant l_1+l_2$ and $M=m_1+m_2$. The functions $G_{\mu l_1 l_2}(R;\alpha)$ are

$$G_{\mu l_1 l_2}(R;\alpha)=(\sin\alpha)^{l_1+1}(\cos\alpha)^{l_2+1}\times(1+x^2)^{2\mu}e^{-ZR\alpha/n_{\mu}}g_{\mu l_1 l_2}(R;\alpha), \tag{19}$$

where $\alpha=2\tan^{-1}(x)$, n_{μ} is the principal quantum number of the hydrogenlike residual ion, and $g_{\mu l_1 l_2}$ is obtained numerically.

TABLE I. Parameters of the Ba^+ semiempirical potential as given in Eq. (2), in atomic units.

ℓ	a_ℓ	b_ℓ	c_ℓ	β_ℓ
0	13.164 317 7	−5.187 746 7	0.400 380 7	0.324
1	9.234 230 25	−2.922 511 2	0.453 506 9	0.324
2	0.807 960 19	−1.518 654 0	0.100 639 9	0.325
⩾3	−54	0.973 787 95	−0.923 412 46	2.492

III. RESULTS AND DISCUSSION

The effective potential of each barium atom valence electron is based on the monovalent cation Ba^+ eigenvalues. The one-electron model potential $\mathcal{U}(r)$ is adjusted[4] in order to match the numerical solutions of the Schrödinger equation to the experimental energy levels.[30,31] As an improvement from the usual functions used as effective potentials,[4] the expressions adopted in this work [Eq. (2)] are angular momentum dependent, with the coefficients shown on Table I. The parameters p and q are defined as follows: if $\ell<3$ then $(p,q)=(2,0)$, else, $(p,q)=(1,1)$. In Fig. 1, the one-electron interactions as a function of the electronic radius are shown for different angular momentum values. The comparison of the corresponding energies with the experimental values shows a very good agreement. The small errors shown on Table II are an indicative of the quality of the results, which is important for the confidence on the effective potential choice.

For the barium atom, the Schrödinger equation will be solved using the two-electron potential of Eq. (1), which only adds to the electron-core interactions the electron-electron repulsion. As discussed in Sec. II, the hyperspherical adiabatic approach is initially applied with the determination of the HS angular basis, which has to be precisely calculated for each value of R in order to generate reliable potential curves and nonadiabatic couplings for the HS radial equa-

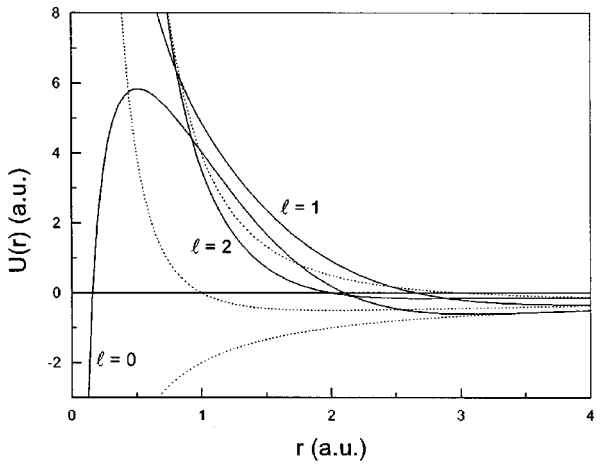

FIG. 1. Model potential $\mathcal{U}(r)$ for the Ba^+ valence electron, compared with the He^+ electron potential.

TABLE II. Monovalent cation Ba^+ energy levels obtained from the Schrödinger equation numerical solution compared with experimental results of Refs. 30 and 31.

Level	$-E$ (a.u.)	$-E_{\text{exp}}$ (a.u.)
$6s$	0.367 635 041	0.367 635 041
$5d$	0.343 238 385	0.343 238 368
$6p$	0.270 180 131	0.270 180 117
$7s$	0.174 649 897	0.174 649 887
$6d$	0.157 711 422	0.157 711 417
$4f$	0.147 166 841	0.147 166 831
$7p$	0.140 709 702	0.140 709 705
$5f$	0.105 514 987	0.105 514 976
$8s$	0.103 251 843	0.103 250 741
$7d$	0.094 904 915	0.094 904 915
$8p$	0.087 231 766	0.087 231 743
$5g$	0.080 451 315	0.080 463 919
$6f$	0.073 039 940	0.073 049 092
$9s$	0.068 358 235	0.068 358 235
$8d$	0.063 705 436	0.063 704 559
$9p$	0.059 511 977	0.059 513 169
$6g$	0.055 853 168	0.055 862 164
$7f$	0.052 153 387	0.052 155 160
$10s$	0.048 625 334	0.048 623 258
$9d$	0.045 779 183	0.045 777 542
$10p$	0.043 225 114	0.043 222 385
$7g$	0.041 018 297	0.041 024 810

tion. These solutions are independent of the energy, which is an advantage for the numerical procedure and spectrum analysis.

The interaction potential term in Eq. (9), $R^2V(R,\Omega)$, contains the radial dependence of the HS angular equation. For R very small this potential is almost null, which implies that the wave function is distributed along α, similarly to a free particle in a box. This state corresponds to the electrons confined closely to the nucleus where the kinetic energy overcomes the potential one. As the value of R increases, the electrons become more sensitive to the interactions, which makes the wave function to locate close to $\alpha=0$ and $\alpha=\pi/2$. When R is very large (more than 10 a.u.), the configuration of the angular solution is that of a bound electron close to the nucleus and the other further away. The full picture of the wave function for large values of R is obtained taking into account the radial solutions, since the HS solution will split in first order as a one-electron bound to the nucleus, which is given by the HS angular solution, and the other also bound to the nucleus, but with a potential screened by the first electron. This second state is given by the solutions of the radial equation.

The hyperspherical potential curves are functions of the maximum value of the individual electronic angular momentum of Eq. (18) coupled in Eq. (11), which we will refer as $\ell_{\max}$. This parameter is also important for the numerical aspect of the work, since the number of coupled equations within the HS angular equation is proportional to the number of configurations. In order to investigate the convergence of Eq. (18), and find the appropriate value of $\ell_{\max}$, a good reference point is the behavior of the first potential curve well minimum, which is a sensitive part for the lower two-electron system bound energies determination. The behavior of such convergence, as seen in Table III, shows that few

TABLE III. Lowest HS potential curve convergence with respect to the maximum value $\ell_{\max}$ of the angular configurations used in the coupled HS angular equation, in Rydbergs.

$\ell_{\max}$	$-U_1(R)/R^2$ (Ry)
0	−1.349 16
1	−1.404 30
2	−1.409 30
3	−1.409 61
4	−1.409 72
5	−1.409 77

configurations give very good results. For large values of R the convergence is faster, which is of great importance for the objective to achieve precise highly excited states. In this work we will proceed the calculations with $\ell_{\max}=4$.

The HS potential curves of the barium atom are shown in Fig. 2, with the dashed lines representing the asymptotic limit of each curve. As R increases, one of the electrons is far from the Ba^+ system, and the potential curve behavior is given by the expansion,

$$-\frac{U_\mu(R)}{R^2}=E[\mathrm{Ba}^+]+\frac{2}{R}+\frac{\lambda}{R^2}+\cdots, \tag{20}$$

where in first order the potential curve are the bound energies of the Ba^+ ion shown in Table II. The second term on the right corresponds to the nuclear potential screened by the inner electron, and the constant λ may be determined by perturbative calculations.[32–36]

With the angular HS channels calculated, the following results derived from the HS angular equation solutions are the nonadiabatic couplings. The most important for bound states, the diagonal coupling Q_{11}, showed in Fig. 3, is responsible for raising the energy from a lower to an upper bound.[12] The contributions of these couplings to the energy are small, reflecting the appropriate choice of the adiabatic coordinate. In the region where the potential curves present anti-crossings, the couplings show peaks, since their calculation involves R derivatives of the channel functions [cf. Eq. (15)]. These peaks, located at small values of R for the curves associated to the lower bound and resonant states, do not reflect on the total wave function, since the radial com-

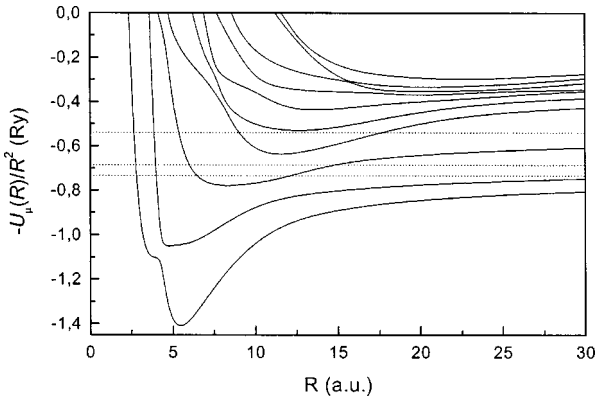

FIG. 2. Hyperspherical potential curves $U_\mu(R)/R^2$ of the barium atom $(L=0, S=0)$.

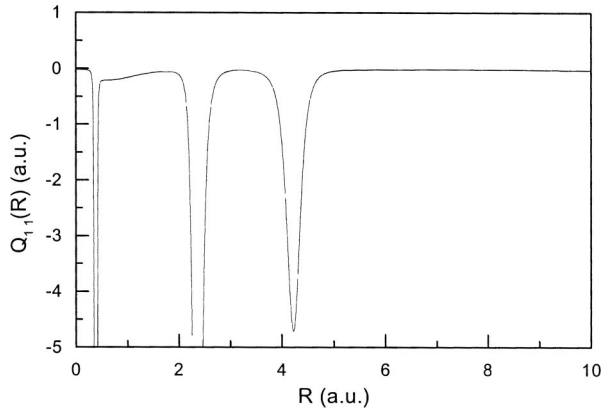

FIG. 3. The diagonal nonadiabatic coupling $Q_{11}(R)$ obtained with the HS angular function of the first potential curve.

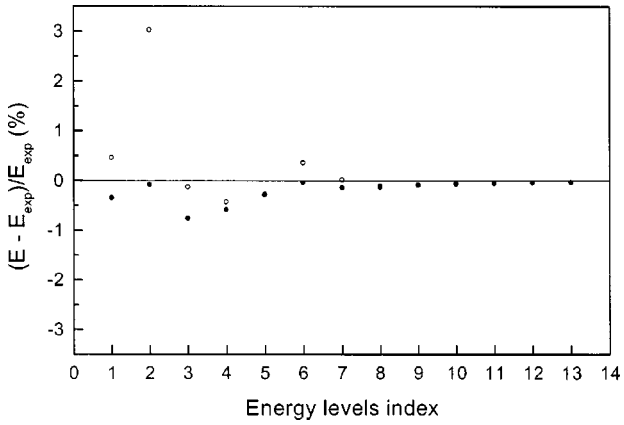

FIG. 4. Comparison between the error of the energy levels, labeled in increasing order, with (dots) and without (open dots) the dielectronic polarization potential term.

ponents of the HS adiabatic expansion [cf. Eq. (12)] acts as a compensation correction in the anticrossing region, resulting in a smooth $R\times\alpha$ wave function surface.[17]

The system bound energies are defined by the lowest potential curve. For energies higher than the first ionization threshold, the channel of the first curve is open, meaning that states on the upper curves are autoionizing. However, by means of the adiabatic approximation, the position of these resonant states may be determined with good results by decoupling the open channels from the radial equation.[16] Such approximation is a valid procedure due to the appropriate choice of the adiabatic variable R, which is related to the moment of inertia of the system, whereas the variable α, related to the relative radial motion of the electrons, represents faster changes on the channel function.

The bound state energies are calculated from the numerical solution of the HS radial equation. The results are shown in Table IV for different numbers of coupled channels. To the first potential curve corresponds the states $6sns$, with $n=6,7,....$ We observe the energies becoming lower as more channels are coupled, approaching the experimental data for the higher states, while for the lower ones the energies surpass them by small amounts. So far, the equations were solved without an effective dielectronic polarization potential,[4] $V_{12}(\mathbf{r}_1,\mathbf{r}_2)$, defined as

$$V_{12}(\mathbf{r}_1,\mathbf{r}_2)=-\frac{\alpha_c}{r_1^2 r_2^2}\cos\theta_{12} f(r_1) f(r_2). \tag{21}$$

With its inclusion, a short-range repulsive effect is added to the potential terms,[3,4,28] dropping the error significantly for the lower states, while keeping the good precision of the excited ones. There is a sensitive improvement of the accuracy of the energies, as seen in Fig. 4. With the inclusion of a larger number of coupled radial channels, the energies would drop, approaching the experimental results. These terms were not took into account, since the effect of higher couplings for two-electron systems is significantly smaller than the first three channel couplings.[21,22]

An interesting characteristic of the barium bound states is the existence of bound doubly excited states. These states are usually coupled with the continuum, lying above the first ionization threshold for simpler two-electron systems like the

TABLE IV. Bound energy levels of the barium atom obtained with one (1C), two (2C), and three (3C) coupled channels in the HS radial equation. The result 3C* is obtained taking the dielectronic polarization term into account.

Level	1C	2C	3C	3C*	Cl[a]	Experimental[b]
$6s^2$	0.537 186	0.553 767	0.561 765	0.557 218	0.558 373	0.559 161
$5d^2$	0.414 449	0.451 459	0.454 639	0.441 612	0.438 390	0.441 270
$6s7s$	0.422 823	0.426 960	0.429 977	0.427 256	0.425 564	0.430 535
$6s8s$	0.397 762	0.399 573	0.400 816	0.400 209	0.401 525	0.402 554
$6s9s$	0.386 767	0.387 729	0.388 459	0.388 381	0.389 173	0.389 510
$6s10s$	0.380 858	0.382 619	0.384 872	0.382 827	0.382 662	0.382 994
$6s11s$	0.377 373	0.381 248	0.381 858	0.381 274	0.379 946	0.381 810
$5d6d$	0.376 438	0.377 662	0.377 994	0.377 875	0.377 896	0.378 401
$6s12s$	0.375 202	0.375 313	0.375 527	0.375 465	0.375 627	0.375 841
$6s13s$	0.373 563	0.373 705	0.373 855	0.373 816	0.373 968	0.374 091
$6s14s$	0.372 450	0.372 557	0.372 664	0.372 637	0.372 765	0.372 843
$6s15s$	0.371 623	0.371 709	0.371 786	0.371 766	0.371 877	0.371 927
$6s16s$	0.370 997	0.371 052	0.371 119	0.371 105	0.371 198	0.371 234

[a]Cl calculations from Férret et Pascale (Ref. 4) (converted from cm^{-1}).
[b]Experimental results from Ref. 30 (converted from cm^{-1}).

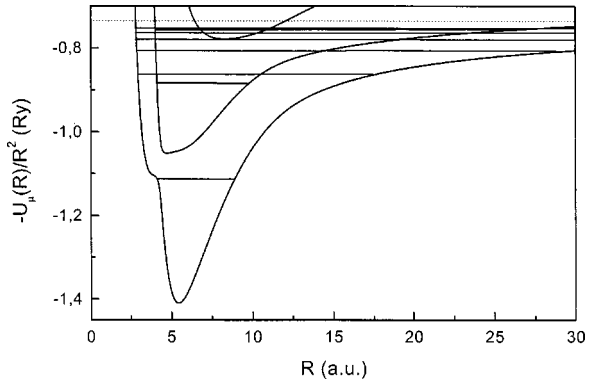

FIG. 5. Bound state energies within the lowest potential curves.

helium atom.[26] With the hyperspherical adiabatic approach such states, $5d^2$ and $5d6d$, are identified within the second potential curve, as observed in Fig. 5, with the state $5d^2$ specially affected by the dielectronic term, as seen on Table V.

The calculation of resonant states within the HS procedure may proceed with bound state procedures uncoupling the open channel of the first potential curve or by the phase shift calculation.

In this work the configurations are relative to $L=0$ and $S=0$ states with spin-averaged coefficients of the Ba^+ ion. States from other configurations may also be calculated. However, it would be necessary to adjust the model potential coefficients[4] in order to account for the spin-orbit coupling effects, which are of great importance for heavy atoms.[37]

IV. CONCLUSION

The hyperspherical adiabatic approach shows a good efficiency for the study of the bound and lower double-excited states of the barium atom. With the HS coordinates, such states, which are very sensitive to the correlation effects, are determined within an intuitive and precise procedure by means of potential curves approach. The adiabatic approach used to solve the Schrödinger equation allows a control for the energy convergence by simple coupling more channels on the HS radial equation. Good quality results are obtained even with the simplest approximation, where the nondiagonal couplings are disregarded.

With respect to the numerical procedures, the energy independence of the potential curves and the existence of only one radial variable is a practical characteristic, which can be explored for the test of different model potentials for alkaline-earth system.

For the ground state energy, the error for the simplest radial approximation was only 4%, which is an indication of the efficiency of the adiabatic separation. The results obtained by coupling more channels on the radial equation, showed the procedure to be comparable to precise CI calculations. Increasing the number of couplings the ground state energy approaches the experimental value, with an error below 0.4% with three coupled channels. The improvement was observed for all states, especially for the highly excited ones. The energy convergence control with quite precise lower and upper bounds with uncoupled radial equations is a significant advantage.

The HAA method has showed to be a good ground test for effective potentials, with fast convergent and precise results, allowing an intuitive insight of the spectra with the use of a Born–Oppenheimer-like adiabatic approximation. The accuracy of the energies also suggests good results for polarizabilities and photodetachment studies using the effective potentials.

TABLE V. Comparison between the error with (3C) and without (3C*) the dielectronic polarization term.

Level	3C	3C*
$6s^2$	0.468	−0.345
$5d^2$	3.032	0.079
$6s7s$	−0.128	−0.760
$6s8s$	−0.430	−0.581
$6s9s$	−0.268	−0.288
$6s10s$	0.362	−0.041
$6s11s$	0.015	−0.138
$5d6d$	−0.105	−0.137
$6s12s$	−0.081	−0.094
$6s13s$	−0.061	−0.070
$6s14s$	−0.046	−0.052
$6s15s$	−0.035	−0.040
$6s16s$	−0.029	−0.031

ACKNOWLEDGMENTS

The authors are grateful to L. Feret and J. Pascale for suggesting this work and gently providing the model potential parameters, and to M. Masili for revising the manuscript. This work was supported by Fundação de Amparo à Pesquisa do Estado de São Paulo (FAPESP, Brazil), under Grant No. 03/05381-0.

[1] M. Aymar, Phys. Rep. **110**, 163 (1984), and references therein.
[2] M. Aymar, C. H. Greene, and Luc-Koenig, Rev. Mod. Phys. **68**, 1015 (1996).
[3] H. W. van der Hart, C. Laughlin, and J. E. Hansen, Phys. Rev. Lett. **71**, 1506 (1993).
[4] L. Féret and J. Pascale, Phys. Rev. A **58**, 3585 (1998).
[5] J. H. Macek, J. Phys. B **1**, 831 (1965).
[6] C. D. Lin, Phys. Rev. A **10**, 1986 (1974).
[7] U. Fano, Phys. Today **29**, 32 (1976).
[8] C. H. Greene, Phys. Rev. A **23**, 661 (1981).
[9] U. Fano, Rep. Prog. Phys. **46**, 97 (1983).
[10] J. E. Hornos, S. W. MacDowell, and C. D. Caldwell, Phys. Rev. A **33**, 2212 (1986).
[11] C. D. Lin and X. Liu, Phys. Rev. A **37**, 2749 (1988).
[12] H. T. Coelho and J. E. Hornos, Phys. Rev. A **43**, 6379 (1991).
[13] J. J. De Groote, J. E. Hornos, H. T. Coelho, and C. D. Caldwell, Phys. Rev. B **46**, 2101 (1992).
[14] H. T. Coelho, J. J. De Groote, and J. E. Hornos, Phys. Rev. A **46**, 5443 (1992).
[15] O. I. Tolstikhin, S. Watanabe, and M. Matsuzawa, Phys. Rev. Lett. **74**, 3573 (1995).
[16] C. D. Lin, Phys. Rep. **257**, 2 (1995), and references therein.
[17] M. Masili, J. E. Hornos, and J. J. De Groote, Phys. Rev. A **52**, 3362 (1995).
[18] S. W. MacDowell and J. J. De Groote, Braz. J. Phys. **26**, 725 (1996).
[19] J. J. De Groote, M. Masili, and J. E. Hornos, J. Phys. B **31**, 4755 (1998).
[20] J. J. De Groote, M. Masili, and J. E. Hornos, Phys. Rev. B **58**, 10383 (1998).

[21] M. Masili, J. J. De Groote, and J. E. Hornos, J. Phys. B **33**, 2641 (2000).
[22] J. J. De Groote, M. Masili, and J. E. Hornos, Phys. Rev. A **62**, 032508 (2000).
[23] A. S. Dos Santos, M. Masili, and J. J. De Groote, Phys. Rev. B **64**, 195210 (2001).
[24] A. S. Dos Santos, J. J. De Groote, and L. Ioriatti, J. Phys.: Condens. Matter **14**, 6841 (2002).
[25] M. A. Cebim and J. J. De Groote, Ecletica Quim. **27**, 67 (2002).
[26] J. J. De Groote and M. Masili, Few-Body Syst. **32**, 249 (2003).
[27] J. P. D'Incão, Phys. Rev. A **67**, 024501 (2003).
[28] J. J. De Groote and M. Masili, J. Chem. Phys. **120**, 2767 (2004).
[29] W. H. Press, S. A. Teukolsky, W. T. Vetterling, and B. P. Flannery, *Numerical Recipes in* FORTRAN77: *The Art of Scientific Computing* (Cambridge University Press, Cambridge, 1992).
[30] C. Moore, *Atomic Energy Levels*, Natl. Bur. Stand. (U.S.) Circ. No. 467 (U.S. GPO, Washingthon, DC, 1958), Vol. 3.
[31] H. Karlsson and U. Litzén, Phys. Scr. **60**, 321 (1999).
[32] S. Hameed, A. Herzenberg, and M. G. James, J. Phys. B **1**, 822 (1968).
[33] I. L. Beigman, L. A. Vainshtein, and P. Shevelko, Opt. Spectrosc. **28**, 229 (1970).
[34] D. W. Norcross, Phys. Rev. A **7**, 606 (1973).
[35] A. Hibbert, Phys. Scr. **39**, 574 (1989).
[36] C. Laughlin, Phys. Scr. **45**, 238 (1992).
[37] P. Hafner and W. H. E. Schwarz, J. Phys. B **11**, 217 (1978).